ESDU 82007

Issued April 1982
Supersedes in part
ESDU 75011
Re-issued March 2012

Structural Members:
mean fluid forces on members of various cross sections

ESDU Copyright material. For current status contact ESDU.

Endorsed by
The Royal Aeronautical Society
Institution of Structural Engineers

Documents
Document Sharing Hub

ESDU DATA ITEMS

Data Items provide validated information in engineering design and analysis for use by, or under the supervision of, professionally qualified engineers. The data are founded on an evaluation of all the relevant information, both published and unpublished, and are invariably supported by original work of ESDU staff engineers or consultants. The whole process is subject to independent review for which crucial support is provided by industrial companies, government research laboratories, universities and others from around the world through the participation of some of their leading experts on ESDU Technical Committees. This process ensures that the results of much valuable work (theoretical, experimental and operational), which may not be widely available or in a readily usable form, can be communicated concisely and accurately to the engineering community.

We are constantly striving to develop new work and review data already issued. Any comments arising out of your use of our data, or any suggestions for new topics or information that might lead to improvements, will help us to provide a better service.

THE PREPARATION OF THIS DATA ITEM

The work on this particular Item was monitored and guided by the Wind Engineering Panel which has the following constitution:

Chairman

Mr T.V. Lawson	—	Bristol University

Members

Prof. A.G. Davenport*	—	University of Western Ontario, Canada
Dr A.R. Flint	—	Flint and Neill
Mr D.H. Freeston*	—	University of Auckland, New Zealand
Mr R.I. Harris	—	Cranfield Institute of Technology
Mr R.A. Lyons	—	Atkins Research and Development
Mr J.R. Mayne	—	Building Research Establishment
Mr R.J. Melling	—	British Telecom
Dr G.A. Mowatt	—	CJB - Earl and Wright Ltd
Mr J.R.C. Pedersen	—	Independent
Mr D.J.W. Richards	—	Central Electricity Research Laboratories
Mr C. Scruton	—	Independent
Mr R.E. Whitbread	—	National Maritime Institute.
Mr G. Wiskin	—	Ove Arup and Partners

* Corresponding Member

The work on this Item was carried out in the Wind Engineering Group of ESDU under the supervision of Mr N. Thompson. The member of staff who undertook the technical work involved in the initial assessment of the available information and the construction and subsequent development of the Item was

Mr B.C. Freeman — Senior Engineer.

ESDU Copyright material. For current status contact ESDU.

Documents
Document Sharing Hub

STRUCTURAL MEMBERS: MEAN FLUID FORCES ON MEMBERS OF VARIOUS CROSS SECTIONS

CONTENTS

		Page
1.	NOTATION AND UNITS	1
1.1	Axis Systems and Force Coefficients	2
2.	PURPOSE, SCOPE AND USE OF THIS DATA ITEM	3
2.1	Purpose and Scope	3
2.2	Applicability, Limitations and Uncertainty	3
2.3	Summary of Calculation Procedure	4
3.	BASIC FORCE COEFFICIENTS	5
3.1	Angle Sections (L-sections)	5
3.2	Channel Sections (U-sections)	5
3.3	H- or I-sections	6
3.4	T-sections	7
3.5	X-sections	7
4.	CORRECTIONS TO THE BASIC DATA	8
4.1	Correction for Finite Aspect Ratio (Free Ends), f_H	8
4.2	Corrections for Yawed Flow, f_β, $f_{Z\beta}$	8
4.3	Correction for Shear Flow	8
4.4	Effects of Reynolds Number	9
4.5	Effects of Turbulence	9
4.6	Effects of Hysteresis	10
4.7	Effects of Interference between Adjacent Members	11
5.	EXAMPLE	12
6.	REFERENCES AND DERIVATION	13
6.1	References	13
6.2	Derivation	14
7.	TABLES	15
7.1	Sources of Experimental Data	15
FIGURES 1 to 19		17 - 34

ESDU Copyright material. For current status contact ESDU.

Documents
Document Sharing Hub
Full document details: ESDU 82007-R1 2012

STRUCTURAL MEMBERS: mean fluid forces on members of various cross sections

1. NOTATION AND UNITS

		SI Unit
A	reference area*, bH	m^2
a	section dimension in $0x$ direction, see Sketch 1.1	m
b	section width in $0y$ direction, see Sketch 1.1	m
C_D	drag coefficient, component along flow direction, see Section 1.1	
C_L	lift or across-flow force coefficient†, component normal to flow direction, see Section 1.1	
C_W	across-flow force coefficient, component normal to the flow direction, see Section 1.1	
C_X	normal force coefficient, component along $0x$ direction, see Section 1.1	
C_Y	lateral force coefficient, component along $0y$ direction, see Section 1.1	
C_Z	longitudinal force coefficient, component along $0z$ direction, see Section 1.1	
D	drag force, force component along flow direction, $\frac{1}{2}\rho V^2 A C_D$	N
f_H	correction factor for effect of finite aspect ratio, see Section 4.1	
f_β , $f_{Z\beta}$	correction factors for effect of yaw, see Section 4.2	
H	length of member along $0z$ direction	m
I_u	intensity of u-component of turbulence, σ_u/V, see Section 4.5	
L	lift force, force component normal to flow direction, $\frac{1}{2}\rho V^2 A C_L$	N
Re_b	Reynolds number based on section dimension b, Vb/ν	
V	time-averaged‡ flow velocity	m/s
W	force component along $0w$ direction, $\frac{1}{2}\rho V^2 A C_W$	N
$0u$, $0v$, $0w$	flow axes, set of right-handed cartesian coordinate axes fixed with reference to mean flow direction, see Section 1.1	

For footnotes see end of Notation Section

Issued April 1982
Re-issued March 2012 – 34 pages

ESDU Copyright material. For current status contact ESDU.
Documents
Document Sharing Hub
Full document details: ESDU 82007-R1 2012

X, Y, Z	body-axis force components, $\frac{1}{2}\rho V^2 A C_X$, $\frac{1}{2}\rho V^2 A C_Y$ and $\frac{1}{2}\rho V^2 A C_Z$ respectively	N
$0x$, $0y$, $0z$	body axes, set of right-handed cartesian coordinate axes fixed with reference to structural member, see Section 1.1	
α	incidence angle, angle between the $0xz$ plane and a plane containing the Oz axis and the flow velocity vector, see Sketch 1.2	degree
β	yaw angle, angle between the $0xy$ plane and a plane containing the $0y$ axis and the flow velocity vector, see Sketch 1.2	degree
ν	kinematic viscosity of fluid	m^2/s
ρ	density of fluid	kg/m^3
Subscripts		
o	basic reference value for two-dimensional, low-turbulence flow	
1, 2, etc.	refer to separate section of stepped structure (Section 4.3)	

* Note that A is independent of the inclination of the flow to the member.

† The symbol C_C is used in some Data Items.

‡ The appropriate averaging time depends on the structure and the design method adopted (see Section 2.2). See Section 4.3 for appropriate value in shear flow.

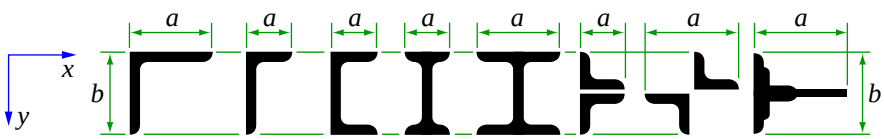

Sketch 1.1 Examples of member cross-sections

1.1 Axis Systems and Force Coefficients

Two systems of axes are widely used in fluid loading studies; (i) a flow-axis system $0u$, $0v$, $0w$, fixed in relation to the mean flow and with $0u$ aligned along the mean flow direction and (ii) a body-axis system $0x$, $0y$, $0z$, fixed in relation to the structure and with $0x$ commonly aligned normal to a principal face of the structure. Whilst the flow-axis system is almost invariably used to describe flow properties, either system may be used to describe the flow-induced forces.

The force coefficient components in the body-axis system are the normal force coefficient C_X and the across-section and along-section force coefficients C_Y and C_Z respectively. The force coefficient components in a flow-axis system are the drag coefficient C_D along the flow direction, $0u$, and across-flow force coefficients C_L (or C_C) and C_W along the $0v$ and $0w$ directions. The force coefficients in the two

ESDU Copyright material. For current status contact ESDU.
Documents
Document Sharing Hub
Full document details: ESDU 82007-R1 2012

systems can be related by:

$$\left.\begin{aligned} C_D &= C_X \cos\alpha\cos\beta + C_Y \sin\alpha - C_Z \cos\alpha\sin\beta \\ C_L &= -C_X \sin\alpha\cos\beta + C_Y \cos\alpha + C_Z \sin\alpha\sin\beta \\ \text{and} \quad C_W &= C_X \sin\beta + C_Z \cos\beta \end{aligned}\right\} \qquad (1.1)$$

where the incidence and yaw angles, α and β, are defined in the Notation and shown in Sketch 1.2.

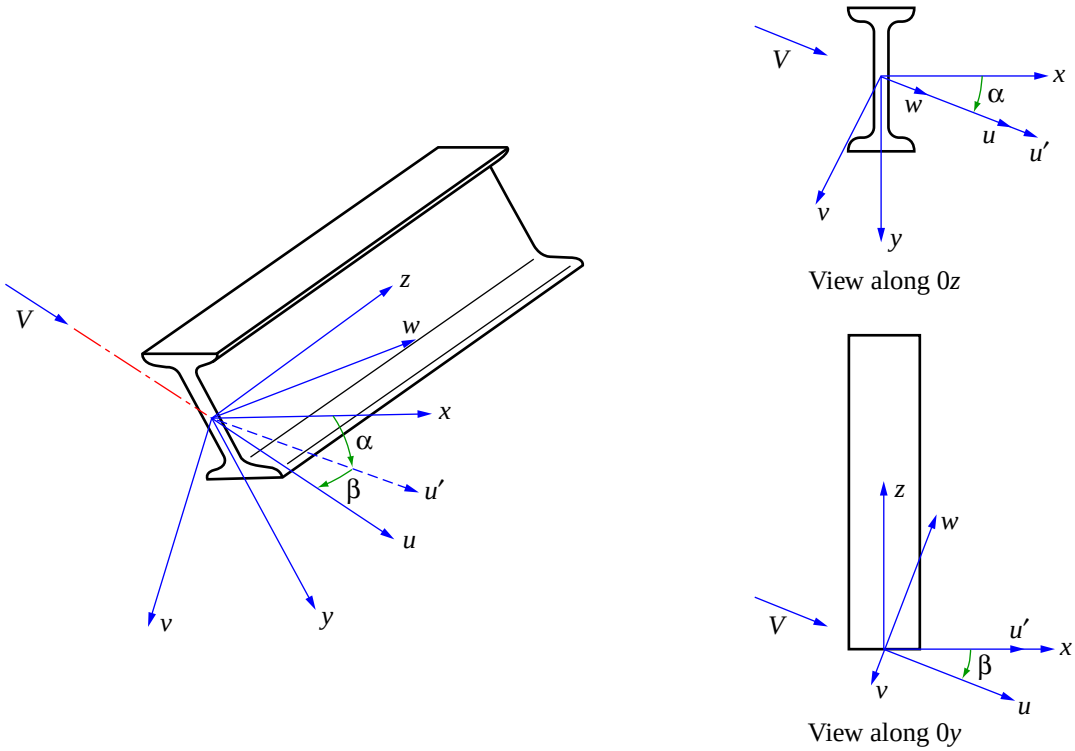

Sketch 1.2

2. PURPOSE, SCOPE AND USE OF THIS DATA ITEM

2.1 Purpose and Scope

This Data Item provides force coefficients for use primarily in estimating mean fluid forces and moments on structural members of sections such as single and compound angles, H- or I-sections, T-sections and channel sections. These data supersede the corresponding information* given in ESDU 75011. The data also have application to other structures of similar cross-sections. Data for rectangular sections are given in References 2 and 6, for circular sections in References 7 and 8 and for polygonal sections in Reference 5.

2.2 Applicability, Limitations and Uncertainty

The Item may be used to estimate the mean loading induced by gas or liquid flows. For gas flows the Mach number should be less than about 0.4. For liquid flows, the possibility of significant forces arising from

* The information on lattice structures in ESDU 75011 is superseded by ESDU 81027 and ESDU 81028.

ESDU Copyright material. For current status contact ESDU.
Documents
Document Sharing Hub
Full document details: ESDU 82007-R1 2012

free-surface effects or from cavitation should be considered separately.

A particular application is to structures in the natural wind. The data may be used to derive the mean component of wind loading (using the mean-hourly wind speed) as part of a statistical approach to the total wind loading. In this approach it is then necessary for design purposes to superimpose the fluctuating components of wind loading on the mean component. The force coefficients from this Data Item may also be used in the calculation procedure of the Data Items in Volume 3a to provide values for the fluctuating components caused by buffeting due to turbulence. The force coefficients may also be used in the calculation of the galloping response of structural members.

The information in this Data Item may also be used in a quasi-static, discrete-gust loading approach in which the total wind loading is assumed to be produced by a discrete gust. In this case the variation of mean wind speed with height is broadly equivalent to that exhibited by a discrete gust sufficiently large to envelope the structure. The time over which the gust velocity is averaged will depend on the structure size; the smaller the structure, the shorter the averaging time and the higher is the gust velocity. Further implications in the discrete-gust loading approach which make it less reliable than the statistical approach are discussed in Section 3.1 of ESDU 81017[8] .

Specific limitations on the application of the data are included as comments in the text or on the Figures. The probable general uncertainty of the data is about ±15 per cent of the values given by the curves, based on the spread of experimental data for the angle section for which most data are available. The data presented are derived largely from tests on rolled steel sections with typical radiused corners as shown in the Sketches. Data for sharp-cornered angle sections (Section 3.1) and H- or I-sections (Section 3.3) follow broadly similar trends but large differences can occur, especially in cross-flow forces. The sources of the experimental data on which the information is based are described briefly in Table 7.1.

2.3 Summary of Calculation Procedure

The mean fluid forces on a structural member are given in terms of body-axis components, by

$$\left.\begin{aligned} X &= \tfrac{1}{2}\rho V^2 A C_X = \tfrac{1}{2}\rho V^2 A C_{Xo} f_H f_\beta , \\ Y &= \tfrac{1}{2}\rho V^2 A C_Y = \tfrac{1}{2}\rho V^2 A C_{Yo} f_H f_\beta , \\ \text{and} \quad Z &= \tfrac{1}{2}\rho V^2 A C_Z = \tfrac{1}{2}\rho V^2 A C_{Xo} f_H f_{Z\beta} . \end{aligned}\right\} \tag{2.1}$$

The mean forces in terms of flow-axis components are given by

$$\left.\begin{aligned} D &= \tfrac{1}{2}\rho V^2 A C_D = \tfrac{1}{2}\rho V^2 A C_{Do} f_H f_\beta , \\ L &= \tfrac{1}{2}\rho V^2 A C_L = \tfrac{1}{2}\rho V^2 A C_{Lo} f_H f_\beta , \\ \text{and} \quad W &= \tfrac{1}{2}\rho V^2 A C_W . \end{aligned}\right\} \tag{2.2}$$

The force coefficients C_{Xo} and C_{Yo}, and C_{Do} and C_{Lo}, are basic coefficients for two-dimensional flow, given in Section 3, and f_H, f_β and $f_{Z\beta}$ are correction factors for the effects of finite length and yaw angle given in Sections 4.1 and 4.2. The force coefficient C_W can be calculated from C_{Xo}, using Equation (1.1) and noting that $C_Z = C_{Xo} f_H f_{Z\beta}$. The effective value of V^2 in a shear flow is derived by integration of the velocity profile as outlined in Section 4.3.

ESDU Copyright material. For current status contact ESDU.

Documents
Document Sharing Hub

Full document details: ESDU 82007-R1 2012

3. BASIC FORCE COEFFICIENTS

This Section presents the basic force coefficients C_{Xo}, C_{Yo}, C_{Do} and C_{Lo} for structural members in a two-dimensional, low-turbulence flow normal to the longitudinal axis of the members, *i.e.*, for zero yaw. The force coefficients C_Z and C_W are zero for this case.

Section 4 considers the effects of departures from the datum conditions, including the effect of yaw angle. The coefficient C_Z is small for all yaw angles but this is not true of C_W (see Equation (1.1)).

3.1 Angle Sections (L-sections)

Figures 1 and 2 present the alternative pairs of force coefficient components C_{Xo} and C_{Yo} and C_{Do} and C_{Lo} for equal-leg angle sections in two-dimensional flow. A typical cross-section is shown in Sketch 3.1. These curves are based primarily on data from Derivations 10, 11, 12, and 14.

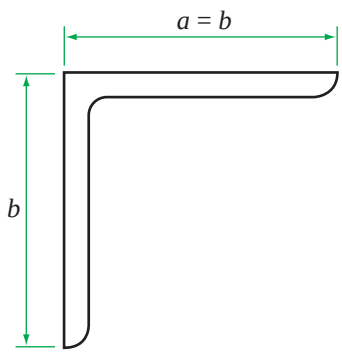

Sketch 3.1

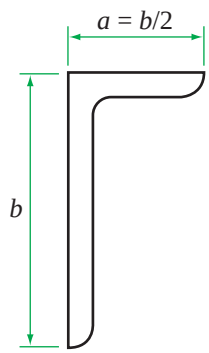

Sketch 3.2

Figures 3 and 4 present the corresponding pairs of force coefficient components for an angle section with one leg half the length of the other, as shown typically in Sketch 3.2. These curves are based on data from Derivation 10 in conjunction with the curves for equal-leg angles. For other leg ratios, interpolation will give some guidance. The shift between incidences at which dominant features of the curves occur should be noted when interpolating.

Derivations 15, 19 and 20 give data for sharp-edged angle sections. Whilst these data follow broadly the trends of Figure 2, large differences in C_{Lo} are present as a result of relatively small changes in the value of α at which peak values occur. Derivations 15 and 19 also include information on torsional moments.

3.2 Channel Sections (U-sections)

Figures 5 and 6 show the force coefficient components C_{Xo}, C_{Yo}, C_{Do} and C_{Lo} for a channel section with flanges of approximately 0.5*b* width. The curves are based on data from Derivations 14 and 17. Derivation 16 quotes a few data for a section with flanges of 0.43*b* which lie within the overall uncertainty of the data.

ESDU Copyright material. For current status contact ESDU.
Documents
Document Sharing Hub
Full document details: ESDU 82007-R1 2012

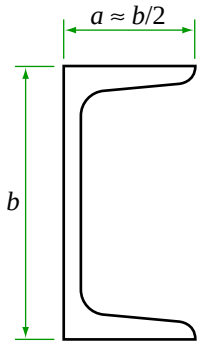

Sketch 3.3

The data for C_{Do} and C_{Xo} from Derivations 14 and 16 show that, for the channel sections tested, these force coefficients decrease significantly with increasing Reynolds number above $Re_b \approx 2 \times 10^5$ for incidences in the range $-180° < \alpha < -130°$. At these incidences the flow is into the channel and it is probable that the separation points vary with Reynolds number as a result of the rounded inner corners of the flanges. On Figures 5 and 6 the solid line applies for $Re_b \leq 2 \times 10^5$ whilst the broken line applies for $Re_b \approx 5 \times 10^5$.

3.3 H- or I-sections

Figures 7 and 8 present force coefficient data for H- or I-sections. The curves for the smaller flange width are based on data from Derivations 10 and 14 and tentative curves for the larger flange width have been interpolated between these data and those of Derivation 21 (for an H-section with a/b = 1.23) on the basis of a few data from Derivations 13 and 16. For other flange widths, approximate values may be obtained by interpolation on Figures 7 and 8.

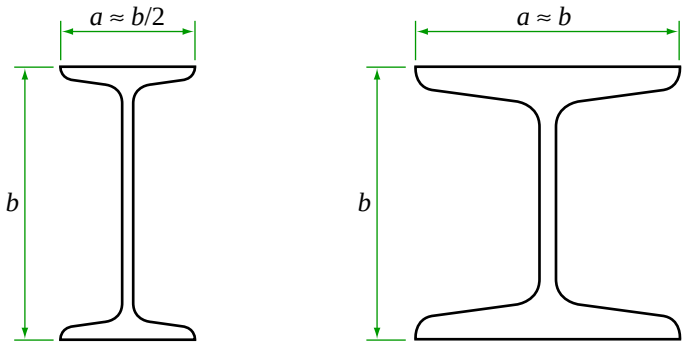

Sketch 3.4

Derivations 20 and 21 present data for sharp-edged H- or I-sections with a/b = 0.64 and 1.23 respectively. The data follow broadly similar trends to Figure 8 when allowance is made for the differences in flange width. The drag coefficient C_{Do} is generally increased by about 15 to 20 per cent above the value expected for a section with rounded edges. It is not possible to generalise the effect on other force coefficients. Derivation 21 also provides torsional moment data for the section with a/b = 1.23.

ESDU Copyright material. For current status contact ESDU.
Documents
Document Sharing Hub
Full document details: ESDU 82007-R1 2012

3.4 T-sections

Figures 9 and 10 present force coefficient data for a T-section built-up from angles and flat strips as in Sketch 3.5. The curves are based on data from Derivation 10. It should be noted that the force coefficients will depend on the ratio of the widths of the flat strips and the data will provide only general guidance for constructions of proportions other than those shown.

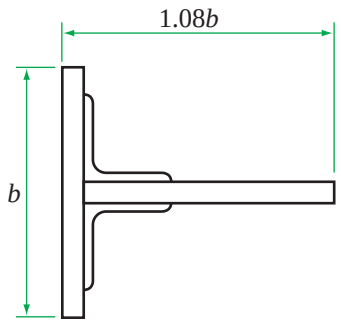

Sketch 3.5

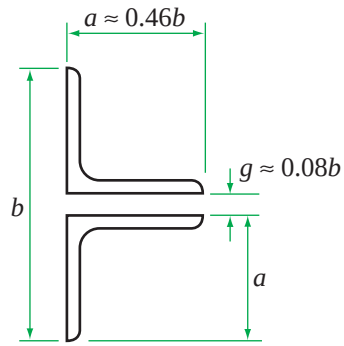

Sketch 3.6

Figures 11 and 12 present the force coefficient components C_{Xo}, C_{Yo}, C_{Do} and C_{Lo} for a compound angle section arranged as a T, as shown in Sketch 3.6, The curves are based on data from Derivation 10. The gap between the angles allows part of the flow through directly into the wake for many incidences, which increases the base pressure (and reduces the drag coefficient) compared with the values that would be obtained for a corresponding solid section. The actual gap depends on the plate thickness used to form the periodic spacers between the angles and the force coefficients will vary with gap width. No data are available from which to assess this variation but its effect is probably small for gaps within about 15 to 20 per cent of that shown, tending to increase C_{Do} as the gap decreases and vice-versa.

3.5 X-sections

Figures 13 and 14 present force coefficients for compound angle sections in an X arrangement, as shown in Sketch 3.7, based primarily on data from Derivation 10. As with T-shaped compound angles, the gap between the angles depends on the spacer plate thickness. Derivation 14 presents data for a section with a smaller gap which suggest that, for this configuration, for α near 0° (and by symmetry near ±90° and ±180°) the force coefficients are increased, whereas for α near ±45° (and ±135°) the force coefficients are decreased from those in Figures 13 and 14. However, the changes were within the expected scatter of the data about the mean curves in Figures 13 and 14.

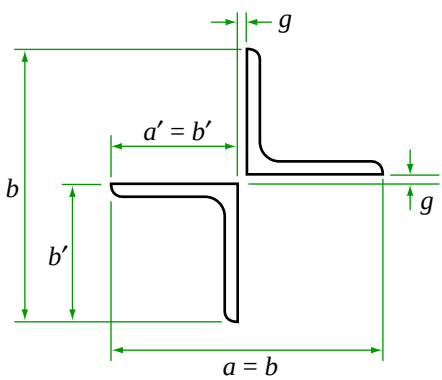

Derivation 10, $b' \approx 0.46b$
$g \approx 0.08b$

Derivation 14, $b' \approx 0.475b$
$g \approx 0.05b$

Sketch 3.7

ESDU Copyright material. For current status contact ESDU.
Documents
Document Sharing Hub
Full document details: ESDU 82007-R1 2012

4. CORRECTIONS TO THE BASIC DATA

4.1 Correction for Finite Aspect Ratio (Free Ends), f_H

The basic data presented in Section 3 apply for two-dimensional flow over structural members long enough for end effects to be negligible (*i.e.*, "infinite aspect ratio"). They can be applied to shorter lengths between end walls and more approximately to any member having other structure attached normal to its ends and extending down-stream, provided that H/b is greater than about 6.

For sections having one* free end, flow around the end reduces the force coefficients. Figure 15 gives a correction factor f_H, for this effect, applicable for zero incidence and yaw angles, as a function of aspect ratio* H/b. Figure 15 is based on extensive data for rectangular sections from Reference 2 together with a few data for angle sections from Derivation 11. The data of Reference 2 suggest a dependence on the value of C_{Do} (or C_{Xo} for $\alpha = 0° = \beta$) for two-dimensional flow which implies that Figure 15 may underestimate f_H by up to 10 per cent for sections with C_{Do} less than about 2, while for $C_{Do} > 2$ it will overestimate.

For $\alpha \neq 0°$, the few data available for angle sections[11] and square sections[2] suggest that f_H from Figure 15 applies approximately to C_D for all incidences for these sections. For other force coefficient components (C_X, C_Y, C_L) the data for square sections[2] suggest that Figure 15 will increasingly overestimate f_H as the force coefficient decreases in magnitude.

For stepped structures such as that considered in Section 4.3 and in the Example, it is suggested that the effective aspect ratios of the two sections, 1 and 2, are taken as $(H_1 + H_2)/b_1$ and $(H_1 + H_2)/b_2$ respectively.

4.2 Corrections for Yawed Flow, f_β, $f_{Z\beta}$

Figure 16 provides an approximate correction factor, f_β, for the effect of yaw angle, β, on the drag coefficient, C_{Do}, for angle sections[11]. In the absence of specific data it is suggested that the correction may be applied to other sections and other force coefficient components (C_{Xo}, C_{Yo} and C_{Lo}) also.

For yawed flow, the force coefficient C_Z along the axis of the section is no longer zero. No specific data were found for this case although Derivation 11 comments that the resultant force was nearly normal to the longitudinal axis of the angle section except near $\beta = 90°$. A tentative factor $f_{Z\beta}$ defined as C_{Zo}/C_{Xo} is given on Figure 16 to indicate a probable order of magnitude of C_Z. The flow-axis force coefficient C_W is also non-zero in yawed flow. If required it may be estimated using Equation (1.1).

4.3 Correction for Shear Flow

It has been found[6] that a simple strip-theory approach gives a good approximation to the overall† mean forces on a structure in a shear flow. This approach assumes that the local force coefficient†, based on local velocity, is constant along a length of structure of constant cross-section. On this basis the overall X-force, for example, on the structure in Sketch 4.1 is given by

* For structures with two free ends the effective aspect ratio is calculated as $\frac{1}{2}H/b$.

† The strip-theory approach will not give reliable results when applied over short lengths of a finite-length structure, especially near the ends. This is because the local force coefficient is, in practice, lower than average along the centre section of the structure, increasing above average near the ends.

ESDU Copyright material. For current status contact ESDU.

Documents
Document Sharing Hub

Full document details: ESDU 82007-R1 2012

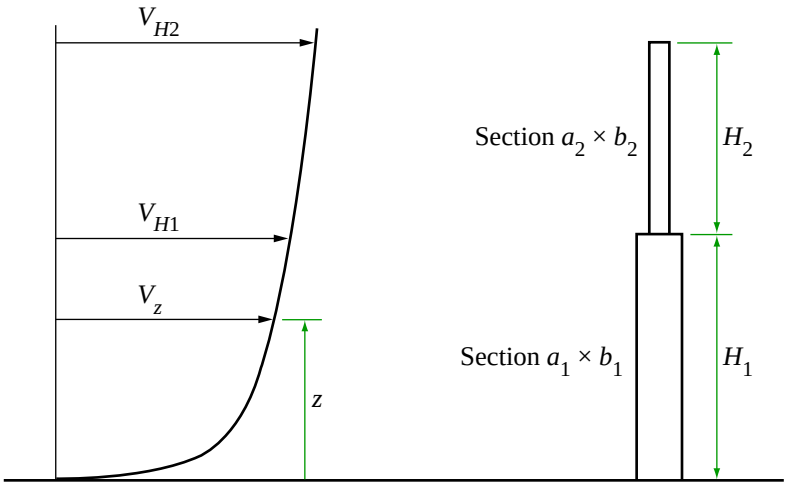

Sketch 4.1

$$X = \int_{z=0}^{z=H_1} \tfrac{1}{2}\rho V_z^2 \; b_1 C_{X1} \mathrm{d}z + \int_{z=H_1}^{z=H_2} \tfrac{1}{2}\rho V_z^2 \; b_2 C_{X2} \mathrm{d}z \tag{4.1}$$

$$= \tfrac{1}{2}\rho \left[\frac{1}{H_1} \int_0^{H_1} V_z^2 \; \mathrm{d}z \right] b_1 H_1 C_{X1} + \tfrac{1}{2}\rho \left[\frac{1}{H_2} \int_{H_1}^{H_2} V_z^2 \; \mathrm{d}z \right] b_2 H_2 C_{X2} \;, \tag{4.2}$$

where the terms in square brackets represent effective mean-squared velocities over the appropriate parts of the shear flow velocity profile. It is usual, for the structures considered here, for the cross-sectional dimensions of the member to be constant over substantial lengths but, if they vary, the variation of b_z with z must be included in the integration of Equation (4.1). The effective aspect ratios for the two sections should be taken as $(H_1 + H_2)/b_1$ and $(H_1 + H_2)/b_2$.

4.4 Effects of Reynolds Number

The data available cover a range of Reynolds numbers of $10^4 < Re_b < 5 \times 10^5$ and suggest that the force coefficients for structural members of the sections covered here are independent of Reynolds number for that range with the exception of those for channel sections. This latter case is discussed in Section 3.2.

4.5 Effects of Turbulence

The information in this Data Item is based on data for low turbulence flows and no detailed quantitative information on effects of turbulence is available. It is evident, however, from data in References 3, 4 and 6 that the effect may be to increase or decrease the force coefficients depending on the section shape, incidence and aspect ratio and on the turbulence level. For example, for rectangular sections in two-dimensional flow, Reference 6 shows a maximum increase in C_X of about 6 per cent at $I_u \approx 4$ per cent and a decrease for $I_u > 7$ per cent. Response data for H-sections[3, 4] suggest a qualitatively similar effect. However, for a rectangular section of an aspect ratio, H/b, of 6 the maximum increase is of the order of 15 to 20 per cent and occurs at $I_u \approx 6$ to 8 per cent and C_X may be increased for all I_u up to about 20 per cent. Figure 17 shows another example of the effect of turbulence, in this case on C_{Yo} for a cruciform section[18]. For all structural sections, the variation of force coefficients with incidence is strongly dependent on the pattern of separation from and reattachment to, the corners and faces and shows indications of hysteresis

ESDU Copyright material. For current status contact ESDU.
Documents
Document Sharing Hub
Full document details: ESDU 82007-R1 2012